Original Article

Interaction of *de novo* cholesterol biosynthesis and Hippo signaling pathway in ductal carcinoma in situ (DCIS)—comparison with the corresponding normal breast epithelium

Danila Coradini^

Laboratory of Medical Statistics and Biometry, "Giulio A. Maccacaro", Department of Clinical Sciences and Community Health, University of Milan, Milan, Italy

Correspondence to: Danila Coradini, PhD. Laboratory of Medical Statistics and Biometry, "Giulio A. Maccacaro", Department of Clinical Sciences and Community Health, University of Milan, Campus Cascina Rosa, Via Vanzetti 5, 20133 Milan, Italy. Email: danila.coradini@gmail.com.

Background: Ductal carcinoma in situ (DCIS) is a non-obligate precursor to invasive breast cancer. However, if left untreated, about 50% of DCIS progress. Preventing such a progression is of paramount importance. Cumulative evidence indicated that the mevalonate cascade, the core of cholesterol biosynthesis, contributes to the regulation of the Hippo signaling pathway providing the isoprenoids required for GTPase activation, the nuclear accumulation of the Yes-associated protein (YAP)/transcriptional coactivator with PDZ-binding motif (TAZ) coactivator, and the subsequent gene transcription and that the disruption of this cooperation associated with tumor progression.

Methods: In this *in silico* study, we investigated whether such a disruption occurred already during the transformation of the normal mammary epithelium into DCIS. To this aim, we interrogated a publicly available dataset, and we explored the interrelationship of the genes involved in the *de novo* cholesterol biosynthesis and the association with those coding for the core components of the Hippo signaling pathway in a set of patient-matched samples of DCIS and corresponding histologically normal (HN) epithelium.

Results: Most genes involved in cholesterol biosynthesis were more expressed in DCIS than in the corresponding HN epithelium. This differential expression was associated with a substantial change in their correlation profile. In particular, 3-hydroxy-3-methylglutaryl coenzyme-A reductase (*HMGCR*) and *INSIG1* lost the positive association shown in the HN epithelium, and their negative association with *LSS* switched to a positive one. Also, *GGPS1*, which plays a crucial role in isoprenoids production, significantly changed its correlation profile. The positive association between *GGPS1* and *HMGCR* or *INSIG1* disappeared, whereas the positive association with *SQLE*, which drives the irreversible commitment to cholesterol, switched to a negative one in DCIS.

Conclusions: Present findings corroborated the hypothesis that a dysfunctional mevalonate pathway possibly concurs with DCIS development by leading to abnormal production of isoprenoids, which in turn activate GTPases and promote YAP/TAZ nuclear translocation, and suggested the safe and low-cost treatment with statins as the possible winning strategy to contrast this metabolic dysfunction.

Keywords: Ductal carcinoma in situ (DCIS); cholesterol biosynthesis; Hippo signaling pathway

Received: 04 August 2023; Accepted: 25 September 2023; Published online: 23 October 2023.
doi: 10.21037/tbcr-23-42
View this article at: https://dx.doi.org/10.21037/tbcr-23-42

^ ORCID: 0000-0003-3771-4341.

Introduction

Ductal carcinoma in situ (DCIS) is an intraductal neoplastic proliferation of epithelial cells without infiltration of the basement membrane (1,2). Since the introduction of mammographic screening in the early 1980s, DCIS incidence has increased dramatically, and at present, it accounts for around 18–25% of newly diagnosed breast tumors (3). Although considered a non-obligate precursor to invasive breast cancer (IBC), if left untreated, about 50% of DCIS progress to IBC even after several decades from diagnosis. Indeed, a 30-year follow-up study showed that 36% of untreated low-grade DCIS progressed to IBC (4,5).

While great efforts have been made to elucidate the molecular journey leading DCIS to IBC with the aim of a more accurate definition of the risk to progress (6-8), less attention has been paid to the molecular and metabolic changes associated with the transformation of the normal mammary epithelium in DCIS. Filling this gap should be very important to identify the early events that trigger and drive this transformation and prevent them.

In the past two decades, accumulating evidence has revealed that Yes-associated protein (YAP) and its homologous transcriptional coactivator with PDZ-binding motif (TAZ) play an essential role in the regulation of many physiological and pathological processes, including tissue homeostasis and regeneration, fibrosis, inflammation, and tumorigenesis (9,10). In particular, YAP/TAZ coactivator proved to be involved in several steps of breast cancer development and progression, including tumor initiation and proliferation, metastatic spread, and drug resistance (11,12).

According to the canonical pathway, the activity of YAP/TAZ is regulated by the Hippo kinases cassette that consists of the serine/threonine kinase 3 (also known as STE20-like kinases MST1), the adaptor protein Salvador family WW domain-containing protein 1 (SAV1), the large tumor suppressor kinase 1 (LATS1) and MOB kinase activator 1A (MOAB1A) (13). As schematically depicted in *Figure 1*, STK kinase in complex with SAV1 directly phosphorylates MOB1A, which in turn, phosphorylates LATS (14). Once activated, LATS phosphorylates YAP/TAZ, thus hampering its migration into the nucleus and promoting its accumulation in the cytoplasm, where YAP/TAZ is degraded (15). Conversely, when unphosphorylated, YAP/TAZ migrates and accumulates into the nuclear compartment, where after binding to the TEA domain transcription factor (TEAD), promotes the transcription of several genes involved in cell proliferation, death, and migration.

Although the Hippo kinases cascade has long been considered the major regulator of YAP/TAZ activity, novel regulatory mechanisms have recently been identified as able to inhibit YAP/TAZ phosphorylation, promote YAP/TAZ nuclear accumulation, and facilitate the interaction with TEAD. The best studied of these regulatory mechanisms is the small GTPase signaling pathway (16). In response to growth factors, acting as a master organizer of cytoskeleton dynamics and assembly of focal adhesions, the small GTPase pathway induces the accumulation of F-actin stress fibers, which, in turn, sequester angiomotin (AMOT), thereby promoting YAP/TAZ activation and nuclear translocation (17) (*Figure 1*). This mechanism was initially supposed as independent of the Hippo pathway, but further studies have demonstrated a link between small GTPase and Hippo pathways: the GTPase pathway can activate YAP/TAZ not only through the F-actin-mediated sequestration of the AMOT but also inhibiting the activity of LATS kinase (18).

To be effective, small GTPases require isoprenylation, a posttranslational modification that allows them to anchor cell membranes and be activated. The failure of small GTPases prenylation results in YAP/TAZ phosphorylation, its binding to AMOT, and degradation.

The main isoprenoids required for GTPases prenylation are farnesyl-pyrophosphate (FPP) and geranylgeranyl-

Highlight box

Key findings

- Most genes involved in cholesterol biosynthesis were more expressed in ductal carcinoma in situ (DCIS) than in the corresponding histologically normal (HN) epithelium. This differential expression was associated with a substantial change in their correlation profile.

What is known and what is new?

- The mevalonate cascade, the core of cholesterol biosynthesis, contributes to the regulation of the Hippo signaling pathway providing the isoprenoids required for GTPase activation, the nuclear accumulation of the YAP/TAZ coactivator, and the subsequent activation of the TEA domain transcription factor (TEAD)-dependent gene transcription.
- Present findings corroborated the hypothesis that a dysfunctional mevalonate pathway concurs with DCIS development.

What is the implication, and what should change now?

- Due to its cholesterol-lowering properties, the safe and low-cost treatment with statins represents a promising strategy to contrast this metabolic dysfunction and DCIS progression.

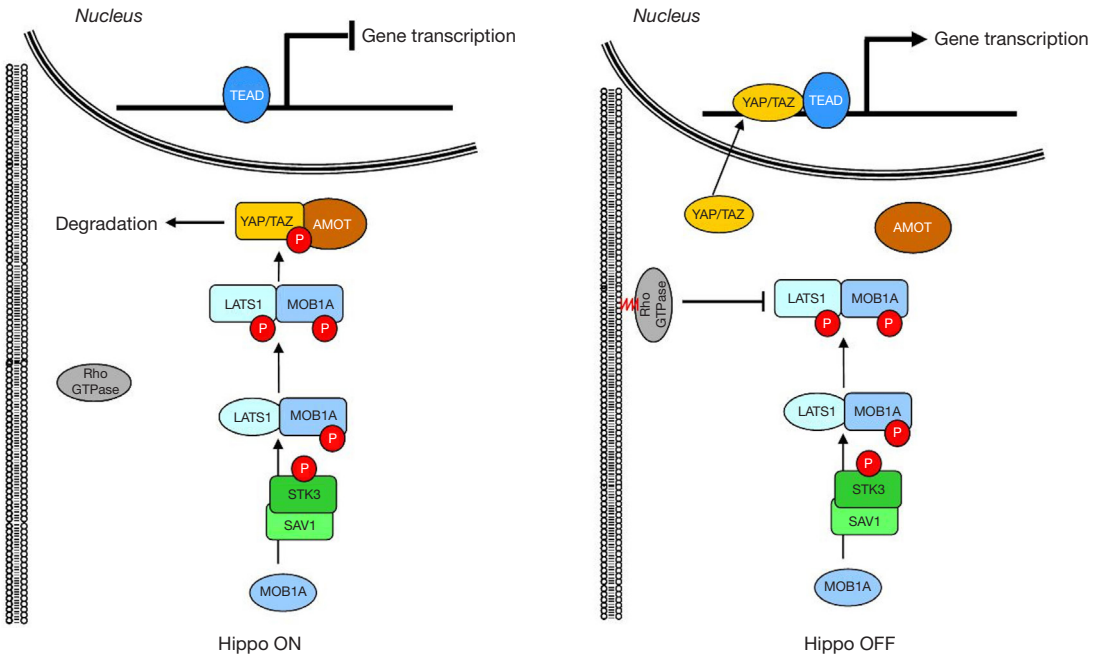

Figure 1 Schematic depiction of the interaction between small GTPase and Hippo signaling pathways. The core of the Hippo pathway consists of a kinase cascade where STK3 in complex with its regulatory protein SAV1, phosphorylates and activates LATS1 in complex with its regulatory protein MOB1A, which, in turn, phosphorylates and inactivates YAP. Phosphorylation of YAP by LATS1 inhibits its translocation into the nucleus, the formation of the complex with TAZ, the binding to TEAD, and the transcription of several genes involved in cell proliferation, death, and migration. TEAD, TEA domain transcription factor; YAP, Yes-associated protein; TAZ, transcriptional coactivator with PDZ-binding motif; AMOT, angiomotin; LATS1, large tumor suppressor kinase 1; MOB1A, MOB kinase activator 1A; STK3, serine/threonine kinase 3; SAV1, Salvador family WW domain-containing protein 1.

pyrophosphate (GGPP), which are produced during the process leading to the *de novo* biosynthesis of cholesterol (*Figure 2*).

The accumulating clinical evidence that cholesterol metabolism is a risk factor for the onset and progression of breast cancer (19) and the experimental finding that cholesterol pathway genes were upregulated during breast cancer progression (20) stimulated the interest for a more accurate elucidation of the relationship among the production of isoprenoids during the cholesterol biosynthesis, Hippo kinase pathway, and YAP/TAZ activity in breast cancer initiation and progression.

In this context, in a very recent study (21), we have shown that in agreement with the hypothesis proposed by Sorrentino *et al.* (22), according to which the mevalonate cascade cooperates in the regulation of the YAP/TAZ activity promoting and sustaining mammary epithelial cells transformation and proliferation, we found that, in IBC, the progressive disruption of this regulatory mechanism associated with tumor grade and worse prognosis.

In the present study, we investigated whether such a disruption occurred already during the transformation of the normal mammary epithelium into DCIS. Therefore, we studied the relationship among the genes involved in the *de novo* cholesterol biosynthesis and those coding for the core components of the Hippo signaling pathway in a set of patient-matched samples of DCIS and corresponding histologically normal (HN) epithelium. We present this article in accordance with the MDAR reporting checklist (available at https://tbcr.amegroups.com/article/view/10.21037/tbcr-23-42/rc).

Methods

Dataset

For this study, we used a dataset publicly accessible at the National Center for Biotechnology Information's Gene Expression Omnibus (GEO) database (http://www.ncbi.nlm.nih.gov/geo/) through the accession number

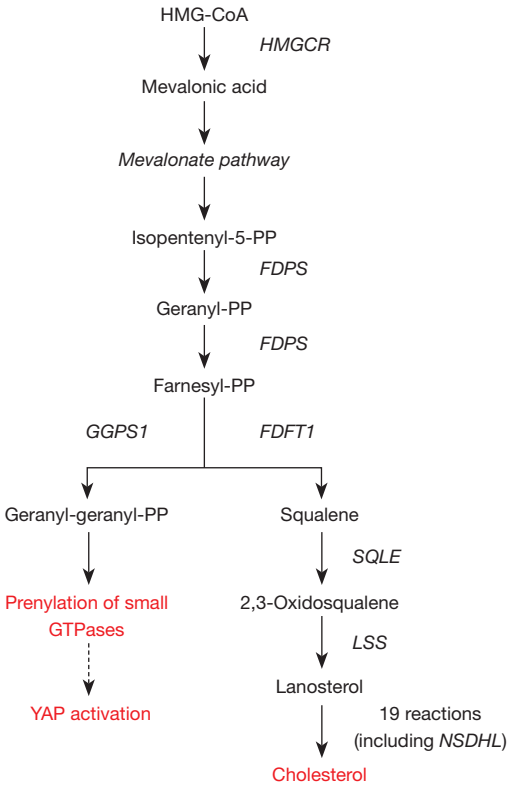

Figure 2 Schematic description of the biosynthetic process that leads to the production of cholesterol and isoprenoids. HMG-CoA, 3-hydroxy-3-methylglutaryl coenzyme-A; *HMGCR*, HMG-CoA reductase; *FDPS*, Farnesyl-PP synthase; *GGPS1*, Geranyl-geranyl-PP synthase; *FDFT1*, Squalene synthase; *SQLE*, Squalene epoxidase; *LSS*, Lanosterol synthase; YAP, Yes-associated protein.

GSE14548, consisting of 18 breast cancer patient-matched samples of DCIS and corresponding HN epithelium. Despite the small number of samples, this dataset was the sole that allowed us to pursue our specific objective: to investigate the relationship between the genes involved in the *de novo* cholesterol biosynthesis and those coding for the core components of the Hippo signaling pathway during the transformation of the normal mammary epithelium into DCIS. Indeed, as described in the original article (23), each sample was processed by laser capture microdissection (LCM) to give highly enriched populations of normal or tumor epithelium. Conversely, in GSE16873, the only accessible dataset containing paired samples of DCIS and corresponding HN tissue, the specimens were epithelial and stroma compartments pooled together.

The original research (23) was approved by the Massachusetts General Hospital human research committee following National Institutes of Health human research study guidelines and deemed exempt from the patient's informed consent as the samples are unidentifiable to the research team. The study was conducted in accordance with the Declaration of Helsinki (as revised in 2013).

Gene set selection

Gene expression was measured using the Affymetrix whole-genome array U133X3P (GEO accession number GPL1352), and the gene expression estimates were provided as filtered and $\log_2$ transformed data. According to the aim of the study, we selected a panel of 16 genes that includes eight genes coding for the most important enzymes involved in cholesterol biosynthesis [3-hydroxy-3-methylglutaryl coenzyme-A (HMG-CoA) reductase (*HMGCR*), *FDPS*, *FDFT1*, *GGPS1*, *SQLE*, *LSS*, and *NSDHL*] and regulation (*INSIG1*); six coding the essential elements of the Hippo pathway [*LATS1*, *MOB1A*, *SAV1*, serine/threonine kinase 3 (*STK3*), *WWTR1*, and *YAP1*]; *BIRC5* and *CDK6*, coding for two recognized direct downstream targets of the YAP-TEAD transcriptional complex, which play a crucial role, in the control of physiologic development of the mammary gland, respectively by coding the antiapoptotic survivin (24), and controlling the cyclin D-CDK4/CDK6 complex during cellular transition from the G1 into the S phase (25) (details on the selected genes in Table S1).

Statistical analysis

Since each gene can be recognized by different probes, thus resulting in numerous gene estimates, we calculated the mean value to obtain single expression data. Wilcoxon paired test was used to assess the differential expression of a given gene in DCIS and the corresponding HN tissue, and Spearman's correlation coefficient was used to describe the correlation between genes. All analyses were performed using the open-source software R Core Team, version 4.1.2 (http://www.R-project.org), and a P value <0.05 was considered statistically significant.

Results

Expression of the genes involved in cholesterol biosynthesis in DCIS and corresponding HN tissue

Wilcoxon paired test showed that all the genes involved in cholesterol biosynthesis were more expressed in DCIS when compared to the corresponding HN tissue, though only

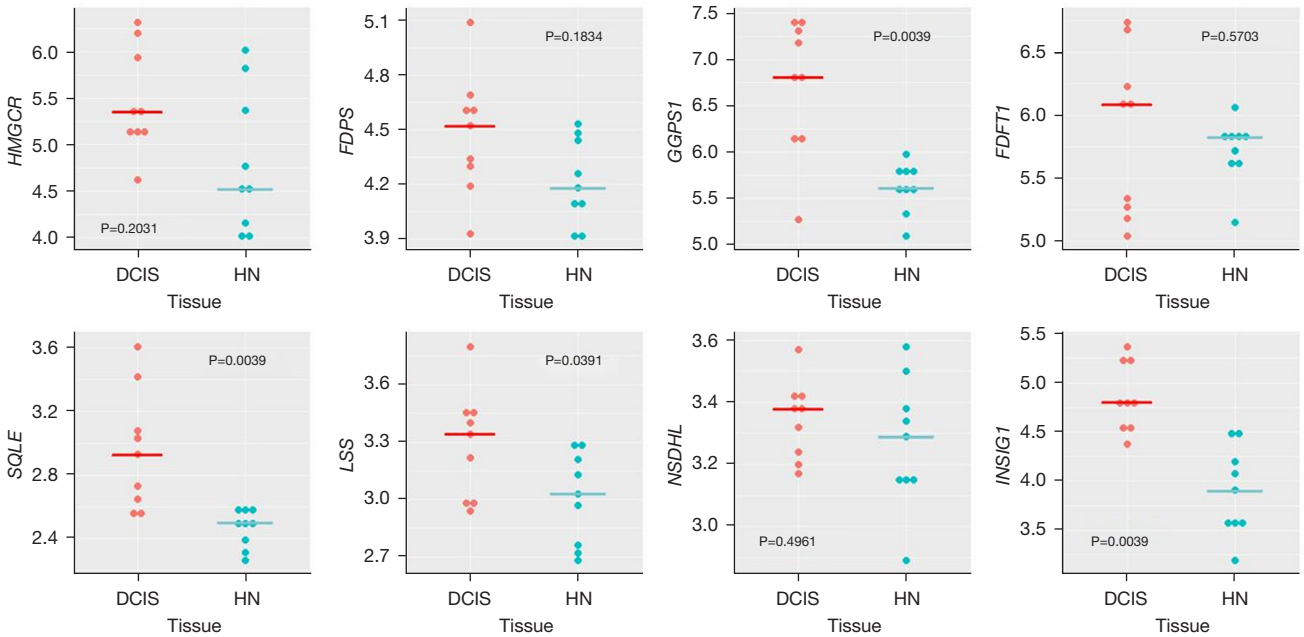

Figure 3 Differential expression of the genes involved in cholesterol biosynthesis in DCIS (in red) and corresponding HN tissue (in blue). P value refers to the Wilcoxon paired test. *HMGCR*, HMG-CoA reductase; HMG-CoA, 3-hydroxy-3-methylglutaryl coenzyme-A; *FDPS*, farnesyl diphosphate synthase; *GGPS1*, geranylgeranyl diphosphate synthase 1; *FDFT1*, farnesyl-diphosphate farnesyltransferase 1; *SQLE*, squalene epoxidase; *LSS*, lanosterol synthase; *NSDHL*, NAD(P) dependent steroid dehydrogenase-like; *INSIG1*, insulin-induced gene 1; DCIS, ductal carcinoma in situ; HN, histologically normal.

GGPS1, *SQLE*, *LSS*, and *INSIG1* reached the statistical significance (*Figure 3*). The correlation analysis indicated that the differential expression of the genes was associated with a substantial change in their interrelationship. As shown in *Figure 4*, the genes more affected by this change were *HMGCR*, which codes for the rate-limiting enzyme in the mevalonate pathway, and *INSIG1*, which codes for the regulatory element of the SREBP-SCAP-Insig complex. Positively associated in HN tissue, *HMGCR*, and *INSIG1* were almost unrelated in DCIS. Besides, their positive association with *GGPS1* or *SQLE* considerably decreased in DCIS compared to the corresponding HN tissue, whereas their negative association with *LSS* switched to a positive one. In addition, *INSIG1* was positively associated with *FDPS* or *FDFT1* in DCIS but not in the corresponding HN tissue. Table S2 shows all the correlations among the genes involved in cholesterol biosynthesis.

Expression of the genes involved in the Hippo signaling pathway in DCIS and corresponding HN tissue and their association with those involved in cholesterol biosynthesis

Wilcoxon paired test showed that, when compared with the corresponding HN tissue, all the genes coding for the essential elements of the Hippo signaling pathway were differentially expressed statistically in DCIS. The expression level of *STK3* and *MOB1A* increased, whereas that of *SAV1* and *LATS1* decreased (*Figure 5*). As regards *YAP1*, *WWTR1*, *BIRC5*, and *CDK6*, while the expression level of *YAP1* and *WWTR1* did not significantly differ between DCIS and HN tissue, that of *BIRC5* and *CDK6* changed in a statistically significant manner: the expression level of *BIRC5* increased while that of *CDK6* decreased (*Figure 5*). The correlation analysis (Table S3) indicated that the positive association of *STK3* with *GGPS1* (r=0.70, P=0.0347) found in HN tissue switched to a negative one (r=–0.85, P=0.0061) in DCIS. Besides, it indicated: a considerable increase in the positive association of *STK3* with *SQLE* as well as of the negative association of *LATS1* with *GGPS1*, a decrease of the positive association of *MOB1A* with *HMGCR*, the appearance of a negative association between *SAV1* and *NSDHL* (r=–0.68, P=0.0503), and a positive association between *MOB1A* and *FDPS* (r=0.62, P=0.0857) (*Figure 6*). As regards *YAP1* and *WWTR1*, the negative association of *YAP1* or *WWTR1* with *LSS* found in NH tissue disappeared in DCIS as well as the positive association of *WWTR1* with *HMGCR*, *GGPS1*, or

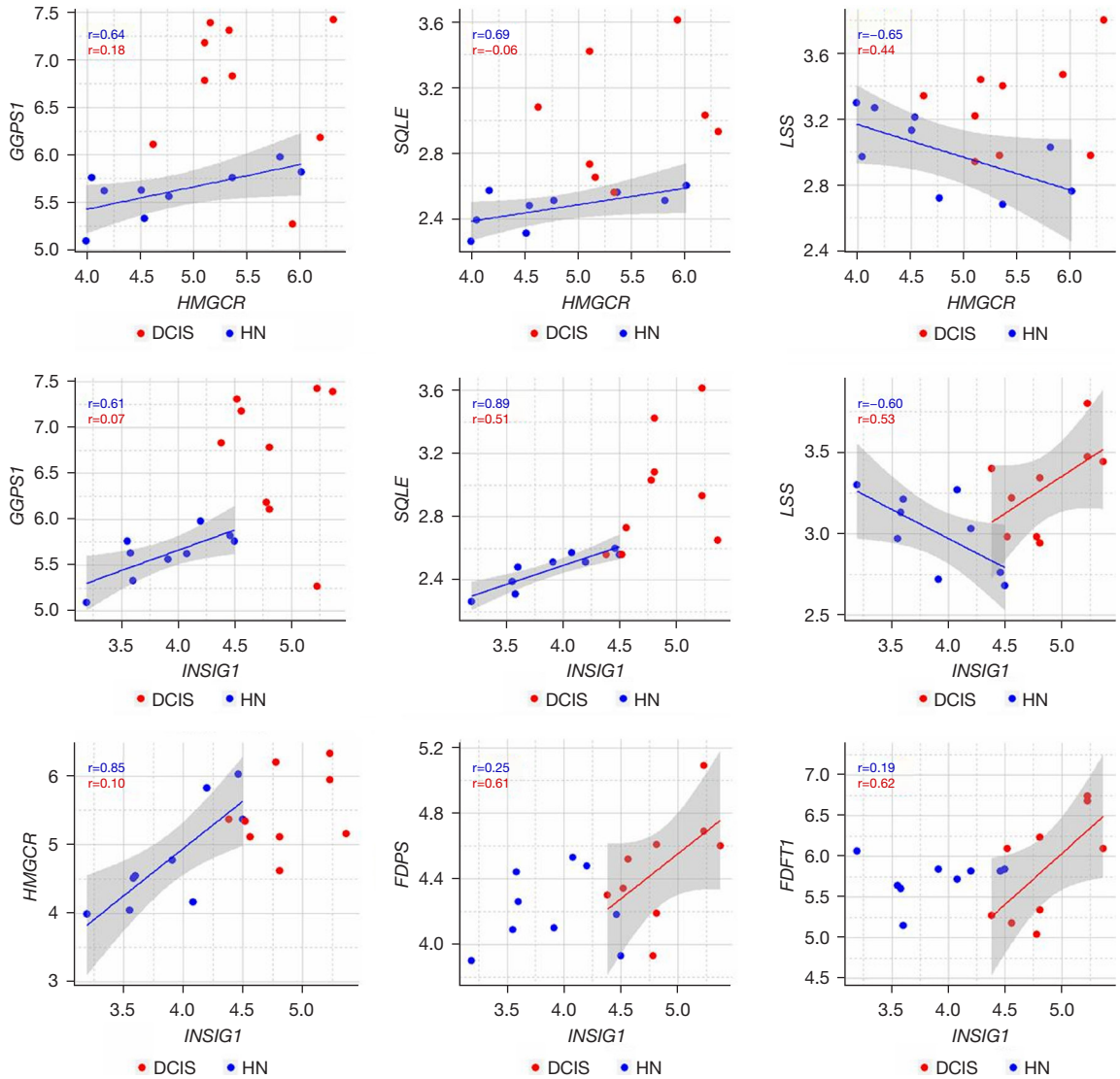

Figure 4 Changes in the relationship among the genes involved in cholesterol biosynthesis. Scatterplots visualize the correlation between *HMGCR* or *INSIG1* and some other genes involved in cholesterol biosynthesis stratified by tissue (HN in blue and DCIS in red). Solid lines represent linear fit from least squares regression. Dark grey shading represents the 95% confidence interval for each solid line. Spearman correlation coefficients (r) are also reported. *GGPS1*, geranylgeranyl diphosphate synthase 1; *HMGCR*, HMG-CoA reductase; HMG-CoA, 3-hydroxy-3-methylglutaryl coenzyme-A; *SQLE*, squalene epoxidase; *LSS*, lanosterol synthase; *INSIG1*, insulin-induced gene 1; *FDPS*, farnesyl diphosphate synthase; *FDFT1*, farnesyl-diphosphate farnesyltransferase 1; DCIS, ductal carcinoma in situ; HN, histologically normal.

INSIG1 (*Figure 6*).

Discussion

Present results indicated that most genes involved in the biosynthetic process leading to the *de novo* production of cholesterol were more expressed in the epithelial compartment of DCIS than the corresponding normal epithelium. The finding agrees with the clinical evidence that the HMG-CoA reductase (evaluated as immunohistochemical cytoplasmic staining) was moderately/strongly expressed in 70% of the assessed DCIS samples (26). Besides, the statistical analysis showed that they modified their interrelationship radically. In particular,

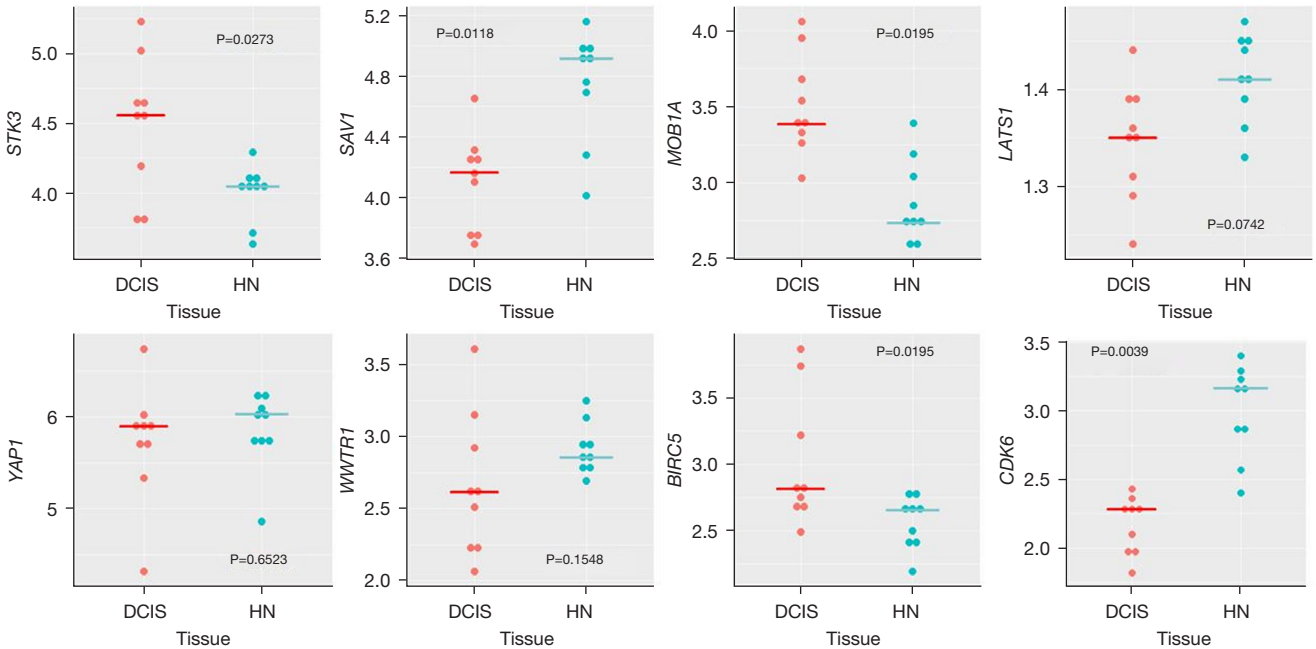

Figure 5 Differential expression of the genes involved in the Hippo signaling pathway in DCIS (in red) and corresponding HN tissue (in blue). P value refers to the Wilcoxon paired test. *STK3*, serine/threonine kinase 3; *SAV1*, Salvador family WW domain containing protein 1; *MOB1A*, MOB kinase activator 1A; *LATS1*, large tumor suppressor kinase 1; *YAP1*, Yes1 associated transcriptional regulator; *WWTR1*, WW domain containing transcription regulator 1; *BIRC5*, baculoviral IAP repeat containing 5; *CDK6*, cyclin dependent kinase 6; DCIS, ductal carcinoma in situ; HN, histologically normal.

HMGCR and *INSIG1*, which code, respectively, for the rate-limiting enzyme in the mevalonate cascade and the regulatory element of the SREBP-SCAP-Insig complex, lose the positive association they had in the HN tissue and substantially changed the relationship with the other genes of the biosynthetic pathway.

Given the role played by cholesterol in cell growth as an essential component in the assembly of new cell membranes and the pivotal function of HMG-CoA reductase and Insig in the regulation of cholesterol production, these results suggest a connection between the disruption of the mechanism that controls the biosynthetic process and the activation, in DCIS, of cell proliferation as indicated by the increased expression of *BIRC5*, which codes for the antiapoptotic survivin (24), and the substantial decrease in the expression level of *CDK6*, which codes for a cyclin-dependent kinase specifically involved in the negative control of the G1-phase of the cell cycle (27). To better understand the basis of such a connection, we remind that in normal tissue, the endogenous production of cholesterol is regulated by the sterol regulatory element-binding protein (SREBP), a membrane-bound transcription factor characterized by a sterol-sensing domain. In the presence of cholesterol, SREBP and its chaperone protein SCAP are retained in the endoplasmic reticulum membrane by the Insig protein. The binding of Insig to the SREBP/SCAP complex prevents the proteolytic generation of the transcriptionally active nuclear form of SREBP, thus limiting the transcription of the *HMGCR* gene and the activation of the downstream mevalonate cascade (28). In addition to the endoplasmic retention of the SREBP/SCAP complex, Insig recruits the HMG-CoA reductase present in the cytosol and promotes its degradation (29) as part of a tightly controlled feedback regulatory system that allows cells to synthesize cholesterol and essential nonsterol isoprenoids while avoiding their toxic overproduction (30).

The functional relationship between Insig and HMG-CoA reductase explains the very similar association profile of *INSIG1* and *HMGCR* with the genes coding for the other component of the biosynthetic process that we found in HN tissue and, in particular, their inverse correlation with *LSS*, the gene coding the 2,3-oxidosqualene-lanosterol cyclase. Also known as lanosterol synthase, this enzyme catalyzes the formation of the sterol nucleus by the cyclization of (S)-

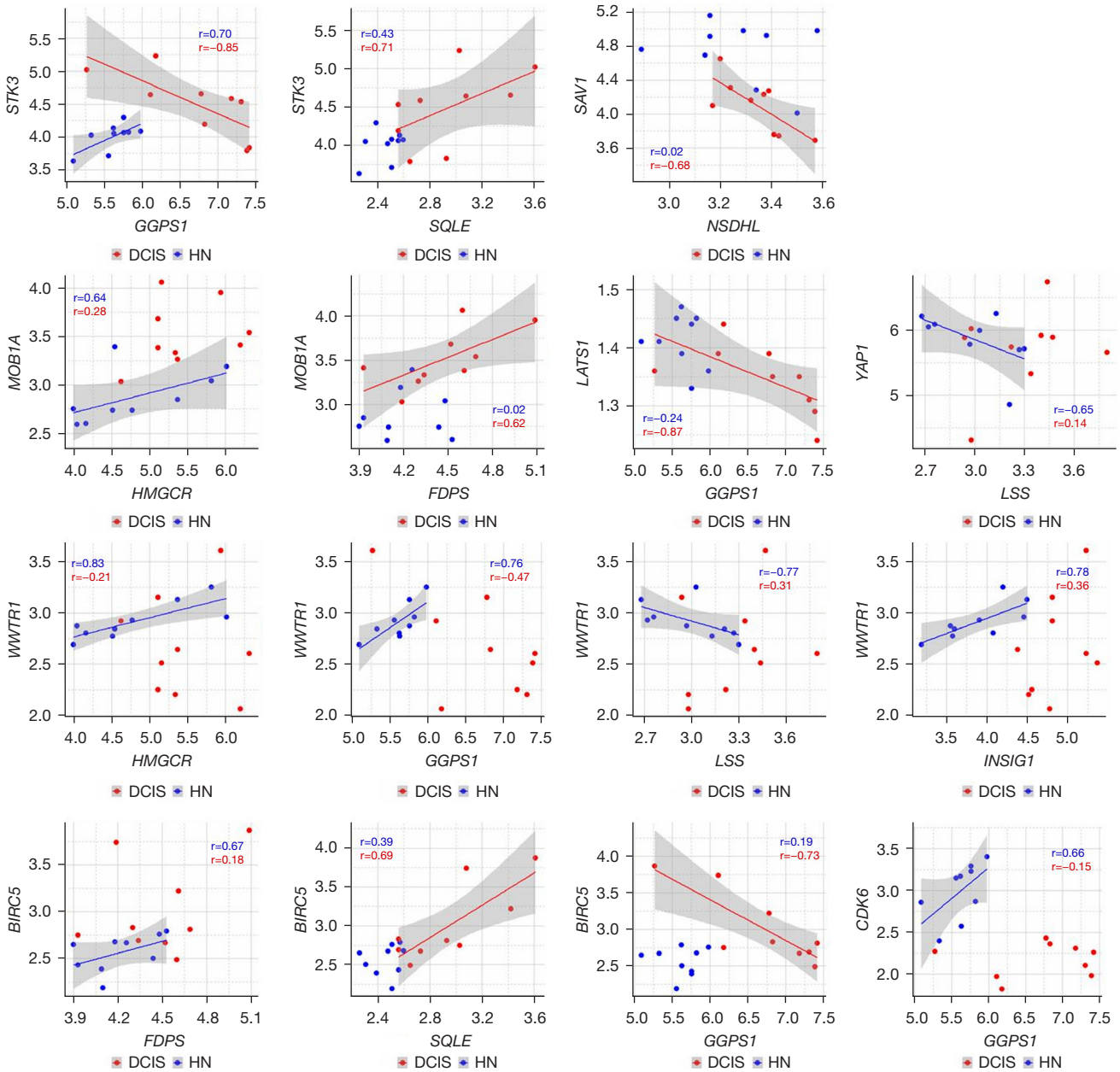

Figure 6 Changes in the relationship among the genes involved in cholesterol biosynthesis and those involved in the Hippo signaling pathway. Scatterplots visualize the correlation between some genes involved in cholesterol biosynthesis (x-axis) and those involved in the Hippo signaling pathway (y-axis) stratified by tissue (HN in blue and DCIS in red). Solid lines represent linear fit from least squares regression. Dark grey shading represents the 95% confidence interval for each solid line. Spearman correlation coefficients (r) are also reported. *STK3*, serine/threonine kinase 3; *GGPS1*, geranylgeranyl diphosphate synthase 1; *SQLE*, squalene epoxidase; *SAV1*, Salvador family WW domain containing protein 1; *NSDHL*, NAD(P) dependent steroid dehydrogenase-like; *MOB1A*, MOB Kinase Activator 1A; *HMGCR*, HMG-CoA reductase; HMG-CoA, 3-hydroxy-3-methylglutaryl coenzyme-A; *FDPS*, farnesyl diphosphate synthase; *LATS1*, Large Tumor Suppressor Kinase 1; *YAP1*, Yes1 associated transcriptional regulator; *LSS*, lanosterol synthase; *WWTR1*, WW domain containing transcription regulator 1; *INSIG1*, insulin-induced gene 1; *BIRC5*, baculoviral IAP repeat containing 5; *CDK6*, cyclin dependent kinase 6; DCIS, ductal carcinoma in situ; HN, histologically normal.

2,3 oxidosqualene to lanosterol, which plays a crucial role in the Insig-mediated degradation of the HMG-CoA (31). The loss of the positive association between *INSIG1* and *HMGCR* and the switch of their negative association with *LSS* to a positive one suggest that the dysfunctional activity of Insig possibly concurs with the development of a DCIS.

The possible causes leading to this dysfunction include a gene mutation in SCAP protein that makes the mutant SCAP resistant to the sterol-mediated conformational change and the binding to Insig much less efficient than the wild-type SCAP (28); epigenetic modifications that inhibit the correct translation of *INSIG1* mRNA (32); posttranslational modifications, such as the Insig phosphorylation at Ser207, that reduce considerably the binding affinity of Insig to sterols or hamper the interaction with SCAP (33); the ubiquitin-dependent degradation of Insig promoted by the hypoxia-induced non-coding circular RNA (circINSIG1) (34). The most convincing of these causes is the microRNAs-mediated posttranscriptional modification of *INSIG1* mRNA since cumulating evidence indicated that microRNA-122 inhibits the synthesis of specific *INSIG1* isoform mRNAs by interfering with the usage of the promoter-proximal cleavage-polyadenylation site leading to the down-regulation of Insig protein (32).

Another interesting finding was the significant change in the correlation profile of *GGPS1*, the gene coding for geranyl-geranyl-PP synthase, which plays a crucial role in isoprenoids production. The positive association between *GGPS1* and *HMGCR* or *INSIG1* disappeared, whereas the positive association with *SQLE*, which codes for the enzyme that catalyzes the synthesis of squalene and the irreversible commitment to cholesterol, switched to a negative one in DCIS. When considered together, these results are of particular interest because they suggested that the disruption of the feedback mechanism that controls the mevalonate pathway lead to the abnormal synthesis of geranyl-geranyl-PP and consequently to increased production of the isoprenoids required for small GTPases anchoring and activation, which in turn, promote YAP nuclear translocation both by the F-actin-mediated sequestration of the AMOT and the inhibition of the LATS kinase activity (17,18). Noteworthy, the high negative association (r=–0.87) between the expression of *GGPS1* and that of *LATS1* suggests that, in addition to the GTPase-mediated inhibition of the LATS kinase activity, geranyl-geranyl-PP may exert negative feedback on the transcription of *LATS1* gene. Once migrated into the nucleus, YAP can form a complex with TAZ and trigger the TEAD-mediated expression of the genes involved in cell proliferation and apoptosis, as supported by the decreased expression of *CDK6* and the increased expression of *BIRC5*.

Of note is the increased expression of the *STK3* and *MOB1A* genes, which code two crucial elements of the Hippo pathway, which appears as an effort to counteract, unsuccessfully, the transcriptional activity of the YAP/TAZ complex.

Unfortunately, the lack of other datasets with characteristics comparable to those of the dataset used in the present study—primarily the availability of epithelium-enriched paired samples of DCIS and corresponding healthy tissue—did not allow us to validate the results in an independent dataset. Indeed, when we interrogated the publicly accessible databases GEO and Array Express, we found several datasets containing DCIS samples and paired or independent IBC samples, very few datasets containing DCIS samples and independent samples of normal tissue, and only one dataset (GSE16873) containing patient-matched samples of DCIS and corresponding HN tissue. But, while the samples used in the present study were epithelial-enriched, those included in dataset GSE16873 contained both epithelial and stromal components that, contributing to a different extent to the gene expression level, would have led to misleading interpretations of the results. Conversely, although obtained in a small number of cases, present findings referred exclusively to the epithelial compartment providing insights on the disruption of the mechanism that regulates cholesterol biosynthesis occurring during the transformation of the normal mammary epithelium into DCIS and characterized by a decreased production of cholesterol, an increased production of isoprenoids and the subsequent promotion of YAP transcriptional activity.

Re-establishing the mechanism that controls cholesterol biosynthesis could represent a promising strategy to restore the correct equilibrium in the production of isoprenoids and cholesterol precursors and prevent the progression of DCIS to IBC due to the inhibition of the Hippo pathway activity. To achieve this, objective different strategies can be adopted, the most feasible of which is the inhibition of the activity of HMG-CoA reductase—the first rate-limiting specific enzyme of cholesterol synthesis—by statins and the activity inhibition of farnesyl pyrophosphate synthase—the regulatory enzyme crucial for the production of isoprenoids—by bisphosphonates. Currently used in clinical practice, respectively, to reduce breast cancer recurrence and mortality (35-37) and for treating patients

with bone-related diseases, including osteoporosis and osteolytic bone metastases (38,39), statins have proven to inhibit the mevalonate pathway and isoprenoids production, thereby hampering the nuclear accumulation of YAP/TAZ complex and its transcriptional function (22) whereas, third-generation amino-bisphosphonates such as zoledronic acid and minodronate, have proved to interfere selectively with farnesyl pyrophosphate synthase thus preventing the biosynthesis of farnesyl pyrophosphate and the downstream geranylgeranyl pyrophosphate (40,41).

The combination of statins and bisphosphonates has been proposed to achieve a synergetic or multifunction effect in diseases related to the accumulation and/or persistence of prenylated proteins in cells (40). Even though no clinical studies have investigated the efficacy of such a combination in cancer disease, adding bisphosphonates to statins could help in counteracting the possible emergence of resistance to statin, as described in a meta-analysis of observational studies (42) and corroborated by the recent *in vitro/in vivo* study by Bhardwaj *et al.* (20) demonstrating that the dysregulation of a panel of genes involved in cholesterol biosynthesis, primarily *HMGCR* overexpression, significantly associated with resistance to statin treatment in mice.

Conclusions

Starting in the early 1980s, the increasing use of mammography screens has increased diagnosis of DCIS, especially among women >50 years of age, where it may represent up to 45% of all new cases of mammographically detected breast cancer (2,43). Although considered a non-obligate precursor to IBC, if left untreated, about 50% of DCIS progress to IBC even after several decades from diagnosis. Preventing such a progression is of paramount importance, and accomplishing this goal in a non-invasive manner represents a clinical challenge. Based on the cumulative evidence, corroborated by the present finding, that DCIS is associated with a dysfunctional mevalonate pathway leading to abnormal production of isoprenoids which in turn promote YAP activation, the safe and low-cost treatment with statins alone or in association with bisphosphonates could represent the winning strategy.

Acknowledgments

Funding: None.

Footnote

Reporting Checklist: The author has completed the MDAR reporting checklist. Available at https://tbcr.amegroups.org/article/view/10.21037/tbcr-23-42/rc

Peer Review File: Available at https://tbcr.amegroups.org/article/view/10.21037/tbcr-23-42/prf

Conflicts of Interest: The author has completed the ICMJE uniform disclosure form (available at https://tbcr.amegroups.org/article/view/10.21037/tbcr-23-42/coif). The author has no conflicts of interest to declare.

Ethical Statement: The author is accountable for all aspects of the work in ensuring that questions related to the accuracy or integrity of any part of the work are appropriately investigated and resolved. The study was conducted in accordance with the Declaration of Helsinki (as revised in 2013).

References

1. Leonard GD, Swain SM. Ductal carcinoma in situ, complexities and challenges. J Natl Cancer Inst 2004;96:906-20.
2. Kuerer HM, Albarracin CT, Yang WT, et al. Ductal carcinoma in situ: state of the science and roadmap to advance the field. J Clin Oncol 2009;27:279-88.
3. Bleyer A, Welch HG. Effect of three decades of screening mammography on breast-cancer incidence. N Engl J Med 2012;367:1998-2005.
4. Collins LC, Tamimi RM, Baer HJ, et al. Outcome of patients with ductal carcinoma in situ untreated after diagnostic biopsy: results from the Nurses' Health Study. Cancer 2005;103:1778-84.
5. Sanders ME, Schuyler PA, Simpson JF, et al. Continued

observation of the natural history of low-grade ductal carcinoma in situ reaffirms proclivity for local recurrence even after more than 30 years of follow-up. Mod Pathol 2015;28:662-9.
6. Schuetz CS, Bonin M, Clare SE, et al. Progression-specific genes identified by expression profiling of matched ductal carcinomas in situ and invasive breast tumors, combining laser capture microdissection and oligonucleotide microarray analysis. Cancer Res 2006;66:5278-86.
7. Tamimi RM, Baer HJ, Marotti J, et al. Comparison of molecular phenotypes of ductal carcinoma in situ and invasive breast cancer. Breast Cancer Res 2008;10:R67.
8. Wiechmann L, Kuerer HM. The molecular journey from ductal carcinoma in situ to invasive breast cancer. Cancer 2008;112:2130-42.
9. Zhao B, Ye X, Yu J, et al. TEAD mediates YAP-dependent gene induction and growth control. Genes Dev 2008;22:1962-71.
10. Zeng Q, Hong W. The emerging role of the hippo pathway in cell contact inhibition, organ size control, and cancer development in mammals. Cancer Cell 2008;13:188-92.
11. Zheng Y, Pan D. The Hippo Signaling Pathway in Development and Disease. Dev Cell 2019;50:264-82.
12. Shi P, Feng J, Chen C. Hippo pathway in mammary gland development and breast cancer. Acta Biochim Biophys Sin (Shanghai) 2015;47:53-9.
13. Yu FX, Guan KL. The Hippo pathway: regulators and regulations. Genes Dev 2013;27:355-71.
14. Praskova M, Xia F, Avruch J. MOBKL1A/MOBKL1B phosphorylation by MST1 and MST2 inhibits cell proliferation. Curr Biol 2008;18:311-21.
15. Zhao B, Li L, Tumaneng K, et al. A coordinated phosphorylation by Lats and CK1 regulates YAP stability through SCF(beta-TRCP). Genes Dev 2010;24:72-85.
16. Ridley AJ, Hall A. The small GTP-binding protein rho regulates the assembly of focal adhesions and actin stress fibers in response to growth factors. Cell 1992;70:389-99.
17. Mana-Capelli S, Paramasivam M, Dutta S, et al. Angiomotins link F-actin architecture to Hippo pathway signaling. Mol Biol Cell 2014;25:1676-85.
18. Jang JW, Kim MK, Bae SC. Reciprocal regulation of YAP/TAZ by the Hippo pathway and the Small GTPase pathway. Small GTPases 2020;11:280-8.
19. Nelson ER. The significance of cholesterol and its metabolite, 27-hydroxycholesterol in breast cancer. Mol Cell Endocrinol 2018;466:73-80.
20. Bhardwaj A, Embury MD, Ju Z, et al. Gene signature associated with resistance to fluvastatin chemoprevention for breast cancer. BMC Cancer 2022;22:282.
21. Coradini D, Ambrogi F, Infante G. Cholesterol de novo Biosynthesis in Paired Samples of Breast Cancer and Adjacent Histologically Normal Tissue: Association with Proliferation Index, Tumor Grade, and Recurrence-Free Survival: De novo cholesterol biosynthesis in breast tissue. Arch Breast Cancer 2023;10:187-99.
22. Sorrentino G, Ruggeri N, Specchia V, et al. Metabolic control of YAP and TAZ by the mevalonate pathway. Nat Cell Biol 2014;16:357-66.
23. Ma XJ, Dahiya S, Richardson E, et al. Gene expression profiling of the tumor microenvironment during breast cancer progression. Breast Cancer Res 2009;11:R7.
24. Martínez-Sifuentes MA, Bassol-Mayagoitia S, Nava-Hernández MP, et al. Survivin in Breast Cancer: A Review. Genet Test Mol Biomarkers 2022;26:411-21.
25. Lucas JJ, Domenico J, Gelfand EW. Cyclin-dependent kinase 6 inhibits proliferation of human mammary epithelial cells. Mol Cancer Res 2004;2:105-14.
26. Butt S, Butt T, Jirström K, et al. The target for statins, HMG-CoA reductase, is expressed in ductal carcinoma-in situ and may predict patient response to radiotherapy. Ann Surg Oncol 2014;21:2911-9.
27. Nebenfuehr S, Kollmann K, Sexl V. The role of CDK6 in cancer. Int J Cancer 2020;147:2988-95.
28. Yang T, Espenshade PJ, Wright ME, et al. Crucial step in cholesterol homeostasis: sterols promote binding of SCAP to INSIG-1, a membrane protein that facilitates retention of SREBPs in ER. Cell 2002;110:489-500.
29. Jo Y, Lee PC, Sguigna PV, DeBose-Boyd RA. Sterol-induced degradation of HMG CoA reductase depends on interplay of two Insigs and two ubiquitin ligases, gp78 and Trc8. Proc Natl Acad Sci U S A 2011;108:20503-8.
30. Luo J, Yang H, Song BL. Mechanisms and regulation of cholesterol homeostasis. Nat Rev Mol Cell Biol 2020;21:225-45.
31. Song BL, Javitt NB, DeBose-Boyd RA. Insig-mediated degradation of HMG CoA reductase stimulated by lanosterol, an intermediate in the synthesis of cholesterol. Cell Metab 2005;1:179-89.
32. Norman KL, Chen TC, Zeiner G, et al. Precursor microRNA-122 inhibits synthesis of Insig1 isoform mRNA by modulating polyadenylation site usage. RNA 2017;23:1886-93.
33. Xu D, Wang Z, Xia Y, et al. The gluconeogenic enzyme PCK1 phosphorylates INSIG1/2 for lipogenesis. Nature 2020;580:530-5.

34. Xiong L, Liu HS, Zhou C, et al. A novel protein encoded by circINSIG1 reprograms cholesterol metabolism by promoting the ubiquitin-dependent degradation of INSIG1 in colorectal cancer. Mol Cancer 2023;22:72.
35. Beckwitt CH, Brufsky A, Oltvai ZN, et al. Statin drugs to reduce breast cancer recurrence and mortality. Breast Cancer Res 2018;20:144.
36. Bjarnadottir O, Romero Q, Bendahl PO, et al. Targeting HMG-CoA reductase with statins in a window-of-opportunity breast cancer trial. Breast Cancer Res Treat 2013;138:499-508.
37. Iannelli F, Lombardi R, Milone MR, et al. Targeting Mevalonate Pathway in Cancer Treatment: Repurposing of Statins. Recent Pat Anticancer Drug Discov 2018;13:184-200.
38. Räkel A, Boucher A, Ste-Marie LG. Role of zoledronic acid in the prevention and treatment of osteoporosis. Clin Interv Aging 2011;6:89-99.
39. Lluch A, Cueva J, Ruiz-Borrego M, et al. Zoledronic acid in the treatment of metastatic breast cancer. Anticancer Drugs 2014;25:1-7.
40. Sun S, McKenna CE. Farnesyl pyrophosphate synthase modulators: a patent review (2006 - 2010). Expert Opin Ther Pat 2011;21:1433-51.
41. Drake MT, Clarke BL, Khosla S. Bisphosphonates: mechanism of action and role in clinical practice. Mayo Clin Proc 2008;83:1032-45.
42. Undela K, Srikanth V, Bansal D. Statin use and risk of breast cancer: a meta-analysis of observational studies. Breast Cancer Res Treat 2012;135:261-9.
43. Sakorafas GH, Farley DR, Peros G. Recent advances and current controversies in the management of DCIS of the breast. Cancer Treat Rev 2008;34:483-97.

doi: 10.21037/tbcr-23-42
Cite this article as: Coradini D. Interaction of *de novo* cholesterol biosynthesis and Hippo signaling pathway in ductal carcinoma in situ (DCIS)—comparison with the corresponding normal breast epithelium. Transl Breast Cancer Res 2023;4:26.

Supplementary

Table S1 Genes selected for the study

Gene symbol	Official gene name	RNA Refseq
Cholesterol biosynthesis		
FDFT1	Farnesyl-diphosphate farnesyltransferase 1	NM_004462
FDPS	Farnesyl diphosphate synthase	NM_002004
GGPS1	Geranylgeranyl diphosphate synthase 1	NM_004837
HMGCR	3-hydroxy-3-methylglutaryl-coenzyme-A reductase	NM_000859
INSIG1	Insulin-induced gene 1	NM_005542
LSS	Lanosterol synthase	NM_002340
NSDHL	NAD(P) dependent steroid dehydrogenase-like	NM_015922
SQLE	Squalene epoxidase	NM_003129
Hippo signaling pathway		
LATS1	Large tumor suppressor kinase 1	NM_004690
MOB1A	MOB (Mps one binder) kinase activator 1A	NM_018221
SAV1	Salvador family WW domain containing protein 1	NM_021818
STK3	Serine/threonine kinase 3	NM_006281
WWTR1	WW domain containing transcription regulator 1	NM_015472
YAP1	Yes1 associated transcriptional regulator	NM_006106
YAP/TAZ-regulated genes		
BIRC5	Baculoviral IAP repeat containing 5	NM_001168
CDK6	Cyclin dependent kinase 6	NM_001259

Refseq, reference sequence; YAP, Yes-associated protein; TAZ, transcriptional coactivator with PDZ-binding motif.

https://dx.doi.org/10.21037/tbcr-23-42

Table S2 Correlation among the genes involved in cholesterol biosynthesis

Gene	HN		DCIS	
	r	P value	r	P value
*HMGCR**				
FDPS	0.23	0.5517	0.20	0.6044
FDFT1	0.10	0.7963	0.24	0.5422
GGPS1†	0.64	0.0610	0.18	0.6354
SQLE†	0.69	0.0412	–0.06	0.8805
LSS†	–0.65	0.0666	0.44	0.2396
NSDHL	–0.06	0.8810	0.13	0.7313
INSIG1†	0.85	0.0061	0.10	0.8038
*FDPS**				
FDFT1	–0.58	0.1017	0.85	0.0034
GGPS1	0.26	0.5003	0.20	0.6134
SQLE	0.33	0.3786	0.34	0.3660
LSS	0.28	0.4630	0.48	0.1942
NSDHL	0.82	0.0068	–0.25	0.5206
INSIG1†	0.25	0.5206	0.61	0.0843
*FDFT1**				
GGPS1	–0.06	0.8715	0.21	0.5890
SQLE	0.11	0.7787	0.32	0.3957
LSS	–0.24	0.5274	0.47	0.2057
NSDHL	–0.73	0.0269	–0.49	0.1854
INSIG1†	0.19	0.6183	0.62	0.0773
*GGPS1**				
SQLE	0.49	0.1832	–0.69	0.0412
LSS	–0.54	0.1301	0.22	0.5739
NSDHL	0.05	0.9060	0.12	0.7756
INSIG1†	0.61	0.0805	0.07	0.8636
*SQLE**				
LSS	–0.46	0.2125	–0.01	0.9914
NSDHL	0.12	0.7548	–0.01	0.9830
INSIG1†	0.89	0.0014	0.51	0.1643
*LSS**				
NSDHL	0.33	0.3914	–0.09	0.8138
INSIG1†	–0.60	0.0968	0.53	0.1407
*NSDHL**				
INSIG1	0.07	0.8641	–0.24	0.5422

The asterisks indicate the correlation between a given gene and the other genes involved in the biosynthetic pathway. †, the associations reported in *Figure 4*. HN, histologically normal; DCIS, ductal carcinoma in situ.

https://dx.doi.org/10.21037/tbcr-23-42

Table S3 Correlation among the genes involved in cholesterol biosynthesis and the Hippo signaling pathway

Gene	HN		DCIS	
	r	P value	r	P value
*HMGCR**				
LATS1	−0.19	0.6183	−0.24	0.5257
MOB1A†	0.64	0.0656	0.28	0.4720
SAV1	−0.04	0.9149	−0.04	0.9149
STK3	0.10	0.8100	−0.02	0.9659
WWTR1†	0.83	0.0083	−0.21	0.5890
YAP1	0.47	0.2125	−0.09	0.8138
*FDPS**				
LATS1	0.20	0.6028	−0.45	0.2296
MOB1A†	0.02	0.9489	0.62	0.0857
SAV1	−0.17	0.6669	0.40	0.2912
STK3	0.42	0.2696	−0.18	0.6436
WWTR1	0.05	0.9116	0.53	0.1475
YAP1	−0.13	0.7435	0.33	0.3853
*FDFT1**				
LATS1	−0.07	0.8624	−0.45	0.2274
MOB1A	0.01	0.9742	0.27	0.4860
SAV1	0.39	0.3019	0.45	0.2220
STK3	−0.37	0.3274	−0.24	0.5292
WWTR1	0.20	0.6028	0.57	0.1098
YAP1	0.20	0.6028	0.28	0.4720
*GGPS1**				
LATS1†	−0.24	0.5257	−0.87	0.0026
MOB1A	0.11	0.7797	0.25	0.5206
SAV1	0.36	0.3454	−0.27	0.4933
STK3†	0.70	0.0347	−0.85	0.0061
WWTR1†	0.76	0.0171	−0.47	0.2125
YAP1	0.50	0.1684	0.37	0.3363
*SQLE**				
LATS1	0.34	0.3680	0.60	0.0854
MOB1A	0.23	0.5497	0.14	0.7150
SAV1	0.34	0.3765	0.18	0.6511
STK3†	0.43	0.2520	0.71	0.0317
WWTR1	0.61	0.0805	0.60	0.0860
YAP1	0.13	0.7476	−0.51	0.1603
*LSS**				
LATS1	0.16	0.6816	−0.57	0.1062
MOB1A	−0.07	0.8641	0.42	0.2624
SAV1	−0.37	0.3296	0.37	0.3296
STK3	−0.15	0.7081	−0.48	0.1942
WWTR1†	−0.77	0.0214	0.31	0.4175
YAP1†	−0.65	0.0666	0.14	0.7150
*NSDHL**				
LATS1	0.05	0.8885	0.17	0.6656
MOB1A	−0.10	0.8047	0.03	0.9484
SAV1†	0.02	0.9658	−0.68	0.0503
STK3	0.44	0.2318	0.10	0.8100
WWTR1	−0.03	0.9316	−0.32	0.4101
YAP1	−0.40	0.2839	−0.63	0.0760
*INSIG1**				
LATS1	−0.12	0.7631	−0.20	0.5997
MOB1A	0.42	0.2624	0.63	0.0688
SAV1	0.35	0.3537	0.39	0.2928
STK3	0.30	0.4366	−0.13	0.7466
WWTR1†	0.78	0.0172	0.36	0.3393
YAP1	0.37	0.3363	0.02	0.9658

The asterisks indicate the correlation between a given gene and the other genes involved in the biosynthetic pathway. †, the associations reported in *Figure 6*. HN, histologically normal; DCIS, ductal carcinoma in situ.

https://dx.doi.org/10.21037/tbcr-23-42